Data dependent concurrent storage sizing and control design for frequency support in isolated power systems

Spyridon Chapaloglou[1], Damiano Varagnolo[2], Francesco Marra[3] and Elisabetta Tedeschi[1,4]

Abstract— As more intermittent energy sources are integrated into isolated power systems, maintaining nominal frequency under the uncertain power fluctuations becomes even more challenging. For that, properly controlled energy storage systems are commonly used to provide frequency support. However, the design of such controllers typically does not rely on system operation data, leading to oversized storage systems and in turn overpriced investments. This paper addresses this problem and presents a methodology for deriving controllers that optimally use a specified storage capability to achieve a target compensation level, given past information of the disturbances. To leverage between uncertainty and actuation (storage) magnitude, the manuscript proposes a data-based approach for deciding alternative combinations of storage size and corresponding control laws that ensure risk constrained robust frequency regulation. The proposed designs are capable of providing additional virtual-inertia services to the isolated system against a guaranteed level of security over all possible uncertainty realizations. An application to an offshore oil and gas platform with onsite gas turbines and locally produced wind power is presented to highlight the numerical properties of the proposed methodology.

I. INTRODUCTION

The operation of modern isolated power systems is becoming less safe and resilient due to the constantly increasing level of converter-interfaced renewable sources (RES) [1]. The problem arises from the combined effects of lower system inertia available to face power fluctuations [2] and uncertainties of the relevant signals [3]. Such effects, that can result in excessive frequency variations, can be attenuated with proper load frequency control (LFC) and storage systems providing virtual-inertia [4].

In this context, to deal with different sources of uncertainty in isolated systems the literature offers a series of robust control strategies based on linearized dynamics. For example, [5]–[7] propose two-degrees of freedom internal model control (IMC) - PID controllers for LFC of power systems, and show that better performance can be achieved compared to conventional PIDs. However, [5]–[7] arbitrarily select the disturbance signals without considering any information related to the system under study. Also model order reduction had to be performed for the control design purpose, leading to simplified estimates of the true dynamics. [8] instead proposes a fractional order PID LFC design via an opportune IMC tuning, leading to better results compared to the aforementioned studies. The design in [8] is shown to be robust enough to be resilient against parametric uncertainties but, as in [5]–[7], no disturbance information was considered in the control design. In addition, in all the above mentioned methodologies, no control saturation limits were considered.

[9] proposes a fractional order fuzzy controller for LFC of a power system that includes storage system. The approach exhibits robust performance under both linear and non-linear operation regimes, the last ones owing to rate limiters. However, this design does not consider inherently those non-linear regimes, and uses simplified probabilistic models for the RES and the load uncertain power signals. [10], instead, proposes a time-varying fuzzy based PI controller that shows improved robustness under different operating conditions. However, also this approach does not inherently consider saturation limits of the specific storage system in the design phase.

Other authors like [11], [12] propose instead H_∞ controllers with the purpose of improving frequency profiles and the virtual-inertia capabilities of storage elements, but omit providing statistical analyses for quantifying the disturbances. Such design methodologies typically consider the performance of a worst-case plant that may never be realized and use over-conservative uncertainty assumptions (norm - bounded descriptions) [13]. However, for power system applications where at least one synchronous generator ensures frequency stability, sizing the storage system for a highly unlikely or even non-realizable worst case, would make any investment economically infeasible. [14] instead considers a simplified statistical model of the disturbances to determine the capacity of a storage system and its effect on frequency control. However, the paper employs simple probability density models that do not capture the time-dependency of the uncertain signals. Other authors then investigate machine-learning oriented strategies: for example [15] employs a deep-learning based control technique, and shows that this approach may lead to marginally slightly better results compared to worst-case based controllers. However, the power disturbance signals are here considered to

[1]Spyridon Chapaloglou and Elisabetta Tedeschi are with the Department of Electric Power Engineering, Norwegian University of Science and Technology, O.S. Bragstads Plass 2 E, 7034 Trondheim, Norway spyridon.chapaloglou@ntnu.no, elisabetta.tedeschi@ntnu.no

[2]Damiano Varagnolo is with the Department of Engineering Cybernetics, Norwegian University of Science and Technology, O.S. Bragstads Plass 2 E, 7034 Trondheim, Norway damiano.varagnolo@ntnu.no

[3]Francesco Marra is with Equinor R&T Electrical Technology department, Arkitekt Ebbels 10, 7005, Trondheim, Norway fmarr@equinor.com

[4]Elisabetta Tedeschi is also with the Department of Industrial Engineering, University of Trento, Via Sommarive, 9, 38123 Povo, Italy

be random, without taking any information of the particular system under study into account.

As it is evident from the aforementioned studies, the existing literature on the LFC design problem usually ignores the physical limits of the system (i.e., the capacity limits of the storage), and this leads to either suboptimal use of the storage or over-conservative control laws. *We here aim at developing a methodology for designing a LFC that is as conservative as needed, and that uses the storage in an efficient way, so that this is not over-sized.* For this reason we employ the scenario approach for control design [16] for the concurrent sizing and control design for a storage system. This is achieved through the use of realistic data of the system under study together with the Variable Robustness Control (VRC) methodology [17]. This enables to explore different robustness levels and gain greater insights into the system uncertainty and leveraging the controller decision against the risk.

Based on the recent breakthroughs in floating offshore wind and the need for cleaner offshore operations (see, e.g., [18]), we consider an isolated offshore Oil and Gas (O&G) platform with significant wind power penetration and a dedicated storage system as a case study for the proposed methodology.

II. METHODOLOGY

The analysed system, whose complete configuration is presented in fig. 1, is composed of: a droop controlled Gas Turbine, a wind farm of 3 identical wind turbines controlled to their maximum power point, and an energy storage system. As field data, we consider time series of aggregated load data and wind speed measurements from a selected offshore location.

A. System modelling

This section describes the linearized small-signal model of the isolated power system. In more details, the power system dynamics are modelled though the commonly used swing equations (see [1]), i.e., as

$$\frac{2H_0}{f_n}\frac{df}{dt} + \frac{D_0}{S_b}f = \frac{P_{imb}}{S_b} \qquad (1)$$

where $H_0\,[s]$ is the rotating mass inertia, $D_0\,[MW/Hz]$ the load dependent damping provided by the various induction

Fig. 1: Schematic configuration of the system analysed in the paper.

motors on the platform, $f\,[Hz]$ the actual frequency of the AC grid, $f_n\,[Hz]$ the nominal one, $S_b\,[MW]$ is the base power and $P_{imb}\,[MW]$ the imbalance power. Considering the Laplace transform of eq. (1) and the variation of imbalance power $P_{imb}\,[MW]$ as the input signal leads to

$$\frac{\Delta f}{\Delta P_{imb}} = G(s) = \frac{1}{2Hs + D}. \qquad (2)$$

Considering the system configuration presented in fig. 1 the complete dynamics are then described by

$$\Delta P_{imb} = \frac{\left(\Delta P_{GT}^* - \frac{1}{R}\Delta f\right)}{(sT_g + 1)(sT_t + 1)} - \Delta P_d + \Delta P_B \qquad (3)$$

$$\Delta P_d = \Delta(P_L - P_{WF}) \qquad (4)$$

where P_L is the load of the power system and P_{WF} the power coming from the wind farm. From eqs. (2) to (4) one can then derive

$$\Delta f = \Delta P_{GT}^* \frac{\dfrac{G(s)}{(sT_g + 1)(sT_t + 1)}}{1 + \dfrac{G(s)}{R(sT_g + 1)(sT_t + 1)}} + \\ (\Delta P_B - \Delta P_d)\frac{G(s)}{1 + \dfrac{G(s)}{R(sT_g + 1)(sT_t + 1)}} \qquad (5)$$

that eventually imply

$$\Delta f = \Delta P_{GT}^* S_r(s) + \left(\Delta P_B - \Delta P_d\right)S_d(s),$$
$$\text{where} \quad S_d(s) = \frac{G(s)}{1 + \dfrac{G(s)}{R(sT_g + 1)(sT_t + 1)}} \qquad (6)$$

is a causal and stable system (invertible). Summarizing, eq. (6) can be considered as the equivalent dynamics of the system under consideration.

Our aim is then to find an outer control loop $C(s)$ that rejects the net load disturbance ΔP_d in eq. (6). For this purpose, we propose to follow a *discrete design* strategy for synthesizing this control law. Thus, we discretize the continuous-time LTI representation $S_d(s)$ through a Tustin approach with a sampling period of $t_s = 0.01\,s$, deemed sufficiently accurate for our purposes, and then design a discrete controller directly on top of the obtained discrete-time system $S_d(z)$. In the following $u(k)$ is the discrete control signal at time step k, indicating the commanded storage power deviation $\Delta P_B(k)$ and $y(k)$ is the output of the plant, indicating the system frequency deviation $\Delta f(k)$. The output feedback controller $C(z)$ shall cancel the dynamics caused by the disturbance. To this aim we use an *Internal Model Controller* approach (see, e.g., [19]) where an the internal plant model is used and for which we require

$$u(k) = Q(z)\Delta P_d(k) \qquad (7)$$

where $Q(z)$ is a strictly stable transfer function. Since the internal model principle outputs proactive control actions using the assumed internal model, [19], the output feedback control action is equivalent to a disturbance feed-forward

action (eq. (7)) from the storage when this is revealed. As for the strictly stable $Q(z)$, we select a commonly used FIR parametrization as in [16] and the control law in eq. (7) can be re-written as

$$u(k) = \Delta P_B(k) = q_0 \Delta P_d(k) + q_1 \Delta P_d(k-1) = \langle \phi_k, \boldsymbol{q} \rangle \quad (8)$$

where $\boldsymbol{q} = [q_0 \quad q_1]^T$ and $\boldsymbol{\phi}_k = [\Delta P_d(k) \quad \Delta P_d(k-1)]^T$.

We then reformulate the robust optimization problem as minimizing the worst-case disturbance effect to our output signal. For this purpose we build our cost function on top of the upper bound h of the commonly used *integral square error* (ISE) of the frequency deviations. Since real-word disturbance dynamics are hard to model, in the proposed approach historical data are used as the best available representation. For that we define the uncertainty set Δ as

$$\delta_i : \{\Delta \boldsymbol{P_d}\}_i, \quad i \in \{1, \dots, N_d\}. \quad (9)$$

as the set of all possible disturbance realizations δ_i (net load deviations profiles $\Delta \boldsymbol{P_d}$, sequences of $\Delta P_d(k)$ values for specified time horizon $t_h = 10\ s$). Realistic wind speed timeseries $v(t, \delta_i)$ were generated from local measurements and a Kaimal filter [20] that models the smaller time scale turbulence related phenomena, after the Normal Turbulence Model [21]. The wind power profiles were calculated through the commonly used cubic power curve transformation, considering the wind turbine dynamics as

$$P_{WF}(v(\delta_i)) = \frac{P_W(v(\delta_i))}{sT_w + 1} \ \forall \ \delta_i \in \Delta. \quad (10)$$

B. Optimization problem formulation

The control design for compensation of frequency fluctuations under uncertain disturbances is cast as the robust optimization problem

$$\begin{aligned} &\underset{h, \boldsymbol{q} \in R^3}{\text{minimize}} \ h \\ &\text{subject to} \quad \sum_{k=1}^{M = \frac{t_h}{t_s}} \Delta f^2(k) \leq h, \forall \ \Delta \boldsymbol{P_d} \in \Delta \\ &\qquad\qquad \left| \Delta P_B(k) \right| \leq \bar{u}, \forall \ k = 0, \dots, t_h. \end{aligned} \quad (11)$$

where $\bar{u}$ is the saturation level of the storage system (i.e., its maximum charge/discharge power rate). Now consider $\Delta P_{GT}^* = 0$, i.e., assume the gas turbine to be scheduled to produce a fixed reference value. Given this assumption we can derive the constraints leveraging on eq. (3), eq. (7) and eq. (8), and obtain

$$\begin{aligned} \sum_{t=1}^{M} y^2(k) &= \sum_{k=1}^{M} [S_d(z)(u(k) - \Delta P_d(k))]^2 = \\ &\sum_{k=1}^{M} [S_d(z)\phi_k^T \boldsymbol{q} - S_d(z)\Delta P_d(k)]^2 \end{aligned} \quad (12)$$

Where we call $\phi_k = [\Delta P_d(k) \quad \Delta P_d(k-1)]^T$, $\psi_k = S_d(z)\phi_k$. In this way eq. (12) becomes

$$\begin{aligned} \sum_{k=1}^{M} y^2(k) &= \sum_{k=1}^{M} \left[\psi_k^T \boldsymbol{q} - S_d(z)\Delta P_d(k) \right]^2 = \\ &\sum_{k=1}^{M} \left(\boldsymbol{q}^T \psi_k \psi_k^T \boldsymbol{q} - 2S_d(z)\Delta P_d(k)\psi_k^T \boldsymbol{q} + (S_d(z)\Delta P_d(k))^2 \right). \end{aligned} \quad (13)$$

Note then that if we choose the decision variables vector as $\boldsymbol{x} = [\boldsymbol{q} \quad h]^T = [q_0 \quad q_1 \quad h]^T$ the constraints of eq. (13) can be rewritten as

$$\boldsymbol{x}^T A \boldsymbol{x} + B \boldsymbol{x} + C \leq 0 \quad (14)$$

where the coefficients A, B and C can be calculated as

$$A = \sum_{k=1}^{M} [\psi_k \quad 0][\psi_k \quad 0]^T$$

$$B = 2\sum_{k=1}^{M} -\Delta P_d(k)S_d(z)[\psi_k \quad 0]^T - [0 \quad 0 \quad 1] \quad (15)$$

$$C = \sum_{k=1}^{M} (-\Delta P_d(k)S_d(z))^2.$$

This means that a quadratic constraint that is formulated from eq. (14) and eq. (15) corresponds to each instance of the uncertain disturbance δ_i. Note though that to calculate the coefficients A, B and C of each of these constraints we first need to simulate the system S_d with the appropriate inputs, a process that we graphically illustrate in fig. 2. Then, based on the scenario approach [22], we can select to disregard a portion of the set of disturbances Δ that from a probabilistic standpoint accounts in total for a probability ε out of the whole probability metric over Δ. This is done by selecting an appropriate number of scenarios N_s so that the optimality of the solution of eq. (11) is $1 - \beta$ level guaranteed against all other unseen instances of uncertainty from Δ. In other words, the designer can select a risk level ε from which she/he can compute a number of scenarios (i.e., constraints) N_s such that the confidence of not violating the unseen constraints is at least $1 - \beta$. The commonly used values $\varepsilon = 0.01$ and $\beta = 10^{-7}$ were selected for this study. Finally, the optimization problem is set as

$$\begin{aligned} &\underset{\boldsymbol{x} \in R^3}{\text{minimize}} \ c^T \boldsymbol{x} \\ &\text{subject to} \\ &\{\boldsymbol{x}^T A \boldsymbol{x} + B\boldsymbol{x} + C\}_i \leq 0, \ \forall \ \delta_i \in \Omega, \quad (16) \\ &\left\{ \left| \begin{bmatrix} \phi_k \\ 0 \end{bmatrix}^T \boldsymbol{x} \right| \leq \bar{u} \right\}_i, \ \forall \ \delta_i \in \Omega, \ k = 0, \dots, t_h. \end{aligned}$$

where $\boldsymbol{x} = [\boldsymbol{q} \quad h]^T = [q_0 \quad q_1 \quad h]^T$ and $c = [0 \quad 0 \quad 1]^T$. Note that the quadratically constrained problem (QCP) eq. (16) can be numerically solved using standard numerical solvers. More specifically, to derive the constraints in eq. (14) we used the *Matlab-Simulink* parallel computing toolbox [23] and solved eq. (16) with the commercial mathematical optimization solver *Gurobi 9.0.3* [24].
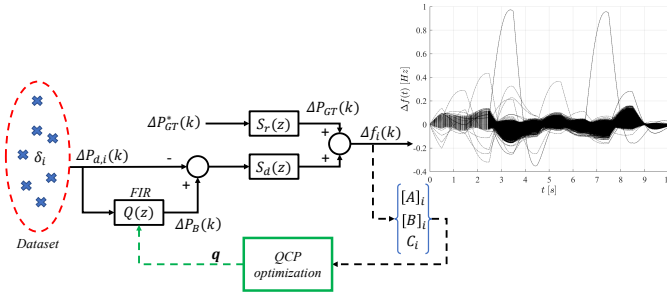
Fig. 2: Graphical summary of the proposed methodology.

TABLE I: Summary of the control design results

$\overline{u}$ [pu]	q_0	q_1	h^*
0.4	1.0023	-0.0023	78.0604
0.3	0.9310	0	78.0642
0.2	0.6206	0	78.1738
0.1	0.3104	0	78.4354
0.09	0.2793	0	78.4699

III. SIMULATION RESULTS

A. Effects of choosing different storage sizes

To investigate the dependency between the control action and the storage capability, we find appropriate controllers $Q(z)$ for different values of the saturation level of the storage system $\overline{u}$. More precisely, we initially set the upper bound to the relatively high value of $\overline{u} = 0.4$, so that basically the storage saturation constraint is not active in eq. (16). The worst case disturbance and the associated control action required $\widehat{u}$ are then presented in fig. 3. Here we can identify the unsaturated peak value of the control action as $\overline{u} = 0.3222 < 0.4$, with the control parameters leading to such design being $q_0 = 1.0023$, $q_1 = -0.0023$ (see also table I) meaning that the full range of the disturbance signals can be counteracted from the proposed storage controller (see also eq. (8)). As can be noticed from fig. 3 such a design is basically able to almost perfectly compensate the worst case disturbance. This means that this controller will also compensate all the other measured disturbances, given the chosen confidence level and risk. Changing the saturation level $\overline{u}$ parameter it is then possible to get different designs that compensate the worst case frequency fluctuations in different ways. The cumulative results, summarized in table I, show that decreasing the saturation level (i.e., choosing a smaller and thus less expensive storage system) increases the optimal value of the ISE performance index h^*. Intuitively,

as $\overline{u}$ diminishes the worst case disturbance first and then, one by one, all the consequent next-worst cases cannot be effectively compensated any more. To this point we note that we observe a distinct pattern: while the q_0 parameter is decreasing as $\overline{u}$ decreases, $q_1 = 0$ most of the times, leading to a controller purely proportional to the disturbance. This indicates that the optimal compensator (QCP optimization eq. (16)), for the particular parametrization (eq. (7)), depends mostly on the present value of the disturbance, and little on the previous one. Despite such a simple controller structure, this is in agreement with the basic *loop-shaping* recommendations for rejecting disturbances entering directly at the plant input [13]. Then, in order to respect the physical saturation limits of the storage, the optimizer selects an appropriate (lower) gain value, meaning that the proportion of the worst disturbance that the specific control design can effectively compensate, is decreased. This effect can be noticed in fig. 4, where we present the results for $\overline{u} = 0.3$. Note that this design is smaller compared to the non-saturated case $\overline{u} = 0.4$; we expect thus that some disturbances will saturate the control output, so that the disturbance will not be perfectly compensated. From fig. 4b we can observe this event, where the controller is saturated just for one case $\widehat{u}$, the one that dominated the initial design. The impact of this effect is presented in fig. 4a, where we compare the corresponding open loop and closed loop outputs y_{ol} and y_{cl}. We can see that even though the worst-case open loop response $\widehat{y}_{ol}$ (depicted in blue) cannot be compensated as effectively as in the other scenarios, the proposed optimal control design leads to a much improved worst-case closed loop response $\widehat{y}_{cl}$ (depicted in red).

B. Effects of choosing different levels of robustness

Based on the results of section III-A, it is evident that for any meaningful storage sizing $\overline{u}$ the control design is dominated by a few specific realizations of the disturbances δ_i. To quantify the effect of these specific δ_i's, and eventually characterize their impact of the data-based uncertainty structure of our problem, we apply the VRC algorithm. For this we employ the Forward Selection Algorithm (FSA) [25] as a means to identify the support scenarios (which are intuitively thought as the ones that are more "different" compared the rest of the sampled dataset) and remove them in turns.

At every iteration k the FSA algorithm preserves the most "equidistant" scenarios, and discards the most "different" ones. The number of the scenarios N_s' to be considered for the VRC algorithm is decided as in [17]. Then, at each iteration k, we can calculate the upper bound ε_k on the probability of

Fig. 3: System response and control action for the worst case scenario - unsaturated design case.
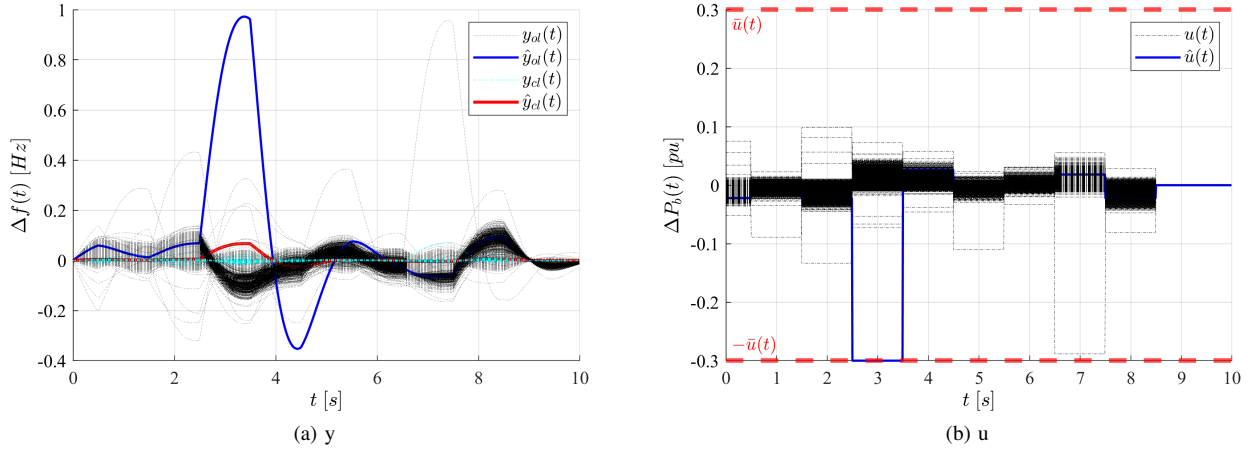
Fig. 4: System response and control action for $\bar{u} = 0.3$.

violating the unseen δ_i instances (i.e., the risk-level) for k removed scenarios out of $N_s{}'$ as

$$\binom{d+k}{k}\sum_{i=0}^{d+k}\binom{N_s{}'}{i}\varepsilon_k^i(1-\varepsilon_k)^{N_s{}'-i} = \frac{\beta}{\bar{k}+1} \ \forall \, k = 0,\ldots,\bar{k} \tag{17}$$

where $d = 2$ is the number of the design variables.

Applying the FSA procedure to the specific case $\bar{u} = 0.09$ leads to the results shown in fig. 5 and table II. From fig. 5 we can observe that as we keep removing scenarios the optimal value h_k^* decreases, while the risk increases from its initial value $\varepsilon = 0.01$. We also note that every time removing a scenario leads to a better solution, this is because a different control design is decided (see also table II). In most cases we get once again $q_1 = 0$, while we find also that the gain q_0 increases for increasing k. This has the following interpretation: as the support scenarios are identified and removed, the storage (whose size is now fixed) can be operated in a way that does not need to

account for (and thus reject) these "bad" realizations of the disturbances. In addition, from table II we can observe that the removal of particular scenarios may have a great effect on the improvement of h_k^*, with the best improvement found at $k = 29$. For our particular system, we see that after that k it is not worth to keep removing scenarios, because the relative improvement is small, at the cost though of increasing risks. Last but not least, it is of high importance to notice from fig. 5 that in general removing a scenario does not necessarily mean improving h_k^*. For example, after $k = 38$ the results did not change. That means that in general there are just a few disturbance scenarios that are dictating the optimal design process; just by increasing our risk we may even neglect them on the initial sizing of the storage system. However, if the storage system is decided (fixed $\bar{u}$), a meaningful risk-averse decision for the controller $Q(z)$ would be $q_0 = 0.7959$ and $q_1 = -0.2131$ with risk level 3.23 times bigger than the initial one.

IV. CONCLUSIONS

This study presents a data-based methodology for the concurrent design of the size and control law of a storage system to be operated in isolated power systems with low inertia and intermittent non-dispatchable energy sources. The results showed that the proposed method can effectively improve the dynamic characteristics of an isolated offshore O&G power system which integrates significant amount of wind power. The proposed design methodology can be considered as a guideline for risk-dependent decision support,
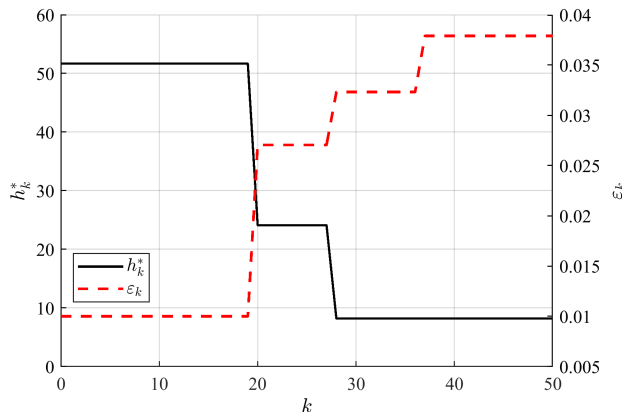
Fig. 5: Dependency of the optimal value h_k^* and of the risk parameter ε_k on the number of scenarios removed through the FSA procedure.

TABLE II: Results about the effects of choosing different levels of robustness

k	q_0	q_1	ε_k [%]	h_k^*	Δh_k^* [%]
0-20	0.3542	0	1.00	51.6588	-
21-28	0.5111	0	2.71	24.1094	-53.33
29-37	0.7959	-0.2131	3.23	8.2075	-65.96
38-79	1.0000	0	3.23	8.1931	-0.18

and for the selection of storage system and its optimal controller, given information specific to the system under study. The case study presented in this paper demonstrates the contribution of appropriately sizing storage to provide frequency support. It is also shown that smaller storage sizes may still effectively compensate uncertain disturbances, at the cost of relatively small risk increment. As future possible work, parametric uncertainty could also be integrated to construct the uncertainty set, while the method could be even used in a rolling horizon way, deciding a control law, given recent past observations and parameters values.

APPENDIX

TABLE III: Summary of the main parameters defining the power system considered in our numerical analyses

Parameter	Value	Units
Base power value	$S_b = 60$	[MW / puMW]
Nominal system frequency	$f_n = 60$	[Hz]
Droop constant	$R = 2.4$	[Hz / puMW]
Power system inertia constant	$H = 0.083$	[puMW s / Hz]
Power system damping constant	$D = 0.0083$	[puMW / Hz]
Governor time constant	$T_g = 0.08$	[s]
Gas turbine time constant	$T_t = 0.3$	[s]
Wind turbine time constant	$T_w = 1.5$	[s]
Nominal wind turbine power	$P_{wt}^n = 15$	[MW]
Number of scenarios in Δ	$N_d = 52560$	[-]
Number of scenarios	$N_s = 2158$	[-]
Number of scenarios for VRC	$N_s' = 2631$	[-]

TABLE IV: Summary of the quantities involved in the models

Variable	Symbol
Platform load	P_L
Wind farm power	P_{WF}
Frequency deviation	Δf
Storage power deviation	ΔP_B
Gas Turbine power deviation	ΔP_{GT}
Net load power deviation	ΔP_d
Imbalance power deviation	ΔP_{imb}
Control action	$u = \Delta P_B$
System output	$y = \Delta f$
Open loop $(S_d(z))$ output	y_{ol}
Closed loop $(S_d(z), C(z))$ output	y_{cl}
Control saturation level	$\bar{u}$
Worst case control action	$\hat{u}$
Worst case system output	$\hat{y}$
Number of removed scenarios	k
Bound of violation probability	ε_k
Optimal ISE upper bound	h_k^*

REFERENCES

[1] K. S. El-Bidairi, H. D. Nguyen, T. S. Mahmoud, S. D. G. Jayasinghe, and J. M. Guerrero, "Optimal sizing of Battery Energy Storage Systems for dynamic frequency control in an islanded microgrid: A case study of Flinders Island, Australia," *Energy*, vol. 195, p. 117059, Mar. 2020.

[2] A. Pepiciello, A. Vaccaro, D. Villacci, and F. Milano, "A Method to Evaluate the Inertial Response of Frequency Controlled Converter-Interfaced Generation," in *2020 IEEE International Conference on Environment and Electrical Engineering and 2020 IEEE Industrial and Commercial Power Systems Europe (EEEIC / I CPS Europe)*, Jun. 2020, pp. 1–6.

[3] Y. Levron and J. Belikov, "Control of Energy Storage Devices Under Uncertainty Using Nonlinear Feedback Systems," p. 5.

[4] H. Golpîra, A. Atarodi, S. Amini, A. R. Messina, B. Francois, and H. Bevrani, "Optimal Energy Storage System-Based Virtual Inertia Placement: A Frequency Stability Point of View," *IEEE Transactions on Power Systems*, vol. 35, no. 6, pp. 4824–4835, Nov. 2020.

[5] Wen Tan, "Unified Tuning of PID Load Frequency Controller for Power Systems via IMC," *IEEE Trans. Power Syst.*, vol. 25, no. 1, pp. 341–350, Feb. 2010.

[6] S. Saxena and Y. V. Hote, "Load Frequency Control in Power Systems via Internal Model Control Scheme and Model-Order Reduction," *IEEE Trans. Power Syst.*, vol. 28, no. 3, pp. 2749–2757, Aug. 2013.

[7] J. Singh, K. Chattterjee, and C. Vishwakarma, "Two degree of freedom internal model control-PID design for LFC of power systems via logarithmic approximations," *ISA Transactions*, vol. 72, pp. 185–196, Jan. 2018.

[8] S. Jain and Y. V. Hote, "Design of fractional PID for Load frequency control via Internal model control and Big bang Big crunch optimization," *IFAC-PapersOnLine*, vol. 51, no. 4, pp. 610–615, 2018.

[9] I. Pan and S. Das, "Fractional order fuzzy control of hybrid power system with renewable generation using chaotic PSO," *ISA Transactions*, vol. 62, pp. 19–29, May 2016.

[10] M.-H. Khooban, T. Niknam, F. Blaabjerg, P. Davari, and T. Dragicevic, "A robust adaptive load frequency control for micro-grids," *ISA Transactions*, vol. 65, pp. 220–229, Nov. 2016.

[11] V. P. Singh, S. R. Mohanty, N. Kishor, and P. K. Ray, "Robust H-infinity load frequency control in hybrid distributed generation system," *International Journal of Electrical Power & Energy Systems*, vol. 46, pp. 294–305, Mar. 2013.

[12] T. Kerdphol, F. S. Rahman, Y. Mitani, M. Watanabe, and S. K. Küfeoğlu, "Robust Virtual Inertia Control of an Islanded Microgrid Considering High Penetration of Renewable Energy," *IEEE Access*, vol. 6, pp. 625–636, 2018.

[13] P. I. Skogestad S., *MULTIVARIABLE FEEDBACK CONTROL Analysis and design*.

[14] H. Jia, Y. Mu, and Y. Qi, "A statistical model to determine the capacity of battery–supercapacitor hybrid energy storage system in autonomous microgrid," *International Journal of Electrical Power & Energy Systems*, vol. 54, pp. 516–524, Jan. 2014.

[15] V. Skiparev, J. Belikov, and E. Petlenkov, "Reinforcement Learning Based Approach for Virtual Inertia Control in Microgrids with Renewable Energy Sources," p. 6.

[16] M. C. Campi, S. Garatti, and M. Prandini, "The scenario approach for systems and control design," *Annual Reviews in Control*, vol. 33, no. 2, pp. 149–157, Dec. 2009.

[17] S. Garatti and M. C. Campi, "Modulating robustness in control design: Principles and algorithms," *IEEE Control Systems Magazine*, vol. 33, no. 2, pp. 36–51, Apr. 2013.

[18] S. Settemsdal, L. Barstad, and W. Voss, "Hybrid power plants can help decarbonize offshore drilling rigs and vessels," p. 4.

[19] J. C. Kantor, "Robust process control. By Manfred Morari and Evanghelos Zafiriou, Prentice-Hall, Inc., Englewood Cliffs, NJ, 1989, 488 pp., $55.00," *AIChE Journal*, vol. 37, no. 12, pp. 1905–1906, 1991.

[20] C. Gavriluta, S. Spataru, I. Mosincat, C. Citro, I. Candela, and P. Rodriguez, "Complete methodology on generating realistic wind speed profiles based on measurements," *REPQJ*, pp. 1757–1762, Apr. 2012.

[21] "INTERNATIONAL STANDARD IEC 61400-1," Tech. Rep. [Online]. Available: http://dlbargh.ir/mbayat/46.pdf

[22] M. C. Campi and S. Garatti, *Introduction to the Scenario Approach*. Philadelphia, PA: Society for Industrial and Applied Mathematics, Nov. 2018.

[23] MATLAB, *9.8.0.1380330 (R2020a) Update 2*. Natick, Massachusetts: The MathWorks Inc., 2020.

[24] L. Gurobi Optimization, "Gurobi optimizer reference manual," 2020. [Online]. Available: http://www.gurobi.com

[25] J. Dupačová, N. Gröwe-Kuska, and W. Römisch, "Scenario Reduction in Stochastic Programming: An Approach Using Probability Metrics," 2003.